

We are IntechOpen, the world's leading publisher of Open Access books Built by scientists, for scientists

6,900

Open access books available

186,000

International authors and editors

200M

Downloads

Our authors are among the

154

Countries delivered to

TOP 1%

most cited scientists

12.2%

Contributors from top 500 universities



WEB OF SCIENCE™

Selection of our books indexed in the Book Citation Index
in Web of Science™ Core Collection (BKCI)

Interested in publishing with us?
Contact book.department@intechopen.com

Numbers displayed above are based on latest data collected.
For more information visit www.intechopen.com



Numerical Analysis of Indoor Air Quality in Hospital Case Study: Bronchoscopy Unit

*Hanaâ Hachimi, Chakib El Mokhi, Badr T. Alsulami
and Abderrahim Lakhout*

Abstract

This paper presents three ventilation scenarios for a bronchoscopy unit using a numerical study. A Fire Dynamics Simulator (FDS) is employed for this purpose. The results obtained are visualized using Smokeview (SMV), which is a program for displaying FDS results. The numerical results are compared with experimental ones from Cheong and Phua's research study. This study was chosen because it investigates ventilation strategies in hospital isolation rooms using a tracer gas technique. In the present work, six points of measurements are utilized to evaluate the concentrations of contaminants and air velocity. The results show that the concentrations estimated by FDS are inferior to the experimental results given by Cheong and Phua. For example, in the SP1 point of measurement, the concentrations estimated by FDS and by Cheong and Phua are 20 and 28.9 ppm, respectively, while in the SP5 point, the concentrations estimated by FDS and by Cheong and Phua are 28.6 and 32.9 ppm, respectively. The error percentages between FDS estimates and experimental measurements made by Cheong and Phua range between 1 and 32%.

Keywords: modelling, indoor air quality, ventilation

1. Introduction

Indoor air quality (IAQ) is an important aspect in the design of buildings due to the effect of IAQ on human health and well-being [1, 2]. In the developed world, people spend about 90% of their time indoors [3], where they are exposed to chemical and biological contaminants and possibly also to carcinogens [4]. Until recently, the health effects of indoor air pollution have received relatively little attention [5].

In particular, the air quality at hospitals carries with it a risk factor for serious health consequences not only for the medical staff but also for patients and visitors. Infection is a common event in hospitals, and many studies have investigated the levels, sources, and characteristics of bioaerosols in these settings [6]. Due to multiple sources of pollution and the presence of vulnerable people, the health sector is particularly at risk of low IAQ [7]. Additionally, outdoor air pollution can affect indoor air quality [8]. Since hospitals are primarily and traditionally a place for people to recover from illness or disease, improving IAQ can help reduce recovery times and thus boost overall productivity [9].

In Europe, more than two million people annually become infected due to healthcare-associated infection (HAI) [10]. Although direct contact is believed to be the main route for transfer of HAI, there is evidence that airborne bacteria may also cause infection due to inhalation [11]. Therefore, it is essential to understand the dynamics of infectious particles that are present in respiratory diseases such as severe acute respiratory syndrome (SARS) and tuberculosis (TB).

This paper examines infection transfer in hospitals caused by poor air quality. To date, only a few researchers have investigated this topic. Cheong and Phua [1] conducted an experimental study on ventilation strategies for improving indoor air quality inside a hospital isolation room, and Qian and Li [12] analyzed ventilation strategies in a hospital isolation chamber using numerical digital tools.

The purpose of the present study is to develop a model for air velocity, temperature profile, and some concentrations of gaseous contaminants in a hospital bronchoscopy unit. Modeling is done using large-eddy simulation (LES). The outcomes of this study will be applied to a hospital in Morocco (North Africa). To validate the work, a hospital in Kenitra, Morocco, has been chosen to measure air quality in the bronchoscopy unit.

2. Materials and methods

To investigate the indoor air quality in the bronchoscopy unit, a Fire Dynamics Simulator was used to simulate the movement of air and the temperature profiles.

2.1 Fire Dynamics Simulator (FDS)

An FDS is a computational fluid dynamics (CFD) model of fire-driven fluid flow. The software described in this document numerically solves a form of the Navier–Stokes equations appropriate for low-air velocity thermally driven flow, with an emphasis on smoke and heat transport from fires.

In this study, the FDS software (version 5) was used. FDS is developed by the National Institute of Standards and Technology (NIST). The first version of FDS was publicly released in February 2000. To date, about half of the applications of the model have been for the design of smoke handling systems and sprinkler/detector activation studies. The other half consists of residential and industrial fire reconstructions [13].

2.2 Hydrodynamic model

The Hydrodynamic Model FDS numerically solves a form of the Navier–Stokes equations, which are appropriate for low-air velocity thermally driven flow, with an emphasis on smoke and heat coming from fires. The core algorithm is an explicit predictor–corrector scheme with second-order accuracy in space and time. Turbulence is treated by means of the Joseph Smagorinsky form of Large-Eddy Simulation. The LES is the default mode of operation [14].

The equations of conservation of mass and momentum written in a system of Cartesian coordinates are as follows [15]:

Equation of conservation of mass:

$$\frac{\partial \rho}{\partial t} + u \cdot \nabla \rho = -\rho \nabla \cdot u \quad (1)$$

where ρ = air density (kg/m^3); u = flow velocity; ∇ = operator nabla.

Equation of conservation of momentum:

$$\frac{\partial u}{\partial t} + u \times \omega + \nabla \mathcal{H} = \frac{1}{\rho} \left((\rho - \rho_0) \vec{g} + f_b + \nabla \cdot \tau_{ij} \right) \quad (2)$$

where \mathcal{H} = pressure; \vec{g} = vector of gravity (m/s²).
Such that:

$$(u \cdot \nabla) u = \frac{\nabla |u|^2}{2} - u \times \omega \quad (3)$$

ω = air velocity component on z (m/s).

$$\mathcal{H} = |u|^2/2 + p/\rho_\infty \quad (4)$$

ρ_∞ = density of ambient air (kg/m³)

$$\delta_{ij} = \begin{cases} 1 & \text{si } i = j \\ 0 & \text{si } i \neq j \end{cases} \quad (5)$$

δ_{ij} = Kronecker delta

$$S_{ij} = \frac{1}{2} \left(\frac{\partial u_i}{\partial x_j} + \frac{\partial u_j}{\partial x_i} \right) \quad (6)$$

S_{ij} = strain tensor symmetric rate.

2.3 Smokeview

Smokeview is a software developed as FDS by NIST. It is used to view the geometry, mesh size, and results obtained by FDS and includes several visualization techniques.

2.4 Geometry of bronchoscopy unit

The studied room, as shown in **Figure 1**, consists of a chamber and a corridor. The chamber measures 4.80 m in length, 3.35 m in width, and 2.5 m in height. It

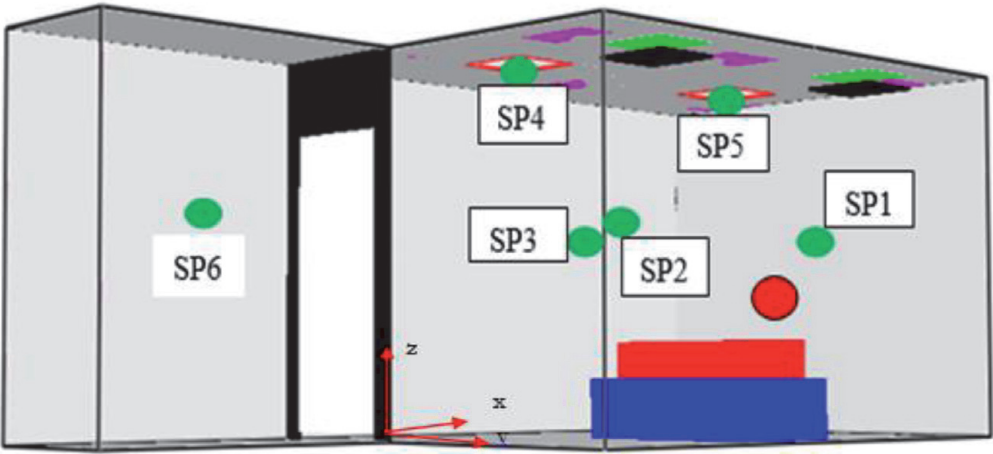


Figure 1.
Geometry of bronchoscopy.

Positions		SP1	SP2	SP3	SP4	SP5	SP6
Coordinates (m)	x	2.30	1.05	2.30	1.50	1.5	0.60
	y	3.90	2.40	1.03	3.90	1.3	−1.32
	z	1.40	1.40	1.40	2.50	2.5	1.40

Table 1.
Position of measurement points in bronchoscopy unit.

contains a bed in the middle. The corridor is 2.65 m long and 1.2 m wide. The corridor is the same height as the chamber.

The room is classified as a high-risk setting (Class 1). According to international standards and the American Society of Heating, Refrigerating and Air Conditioning Engineers (ASHRAE) standards ([16], p. 62), the room must be maintained under negative pressure. This is to prevent any exfiltration of contagious microorganisms or antibiotic-resistant bacteria that may be emitted by a sick patient to other parts of the hospital, as these organisms and bacteria might infect other patients, medical staff, or even visitors.

We use here six points of measure: SP1, SP2, SP3, SP4, SP5, and SP6. These points fall in the plane $z = 1.4$ m (**Table 1**).

2.5 Mesh

For a typical building design simulation using FDS, a large volume of space is simulated. In describing this computation volume, one or more subsections of the overall volume are referred to as a “mesh” and entered as “&MESH” in the FDS input file. In many cases, multiple meshes of different resolutions are required to accurately define the simulated domain. Most modern computers have multiple “cores” or processors per CPU chip, and FDS through the Message Passing Interface (MPI) feature allows for each mesh to be assigned to a specific processor using the MPI_PROCESS keyword. This feature enables any number of meshes to be assigned to the same processor to improve simulation efficiency. In the present study, three different meshes have been tested:

- 1. Dense mesh (DM)
- 2. Less dense mesh (LDM)
- 3. Coarse mesh (CM)

Note that DM has 2.4 times more mesh nodes than LDM and 7.3 times more nodes than CM.

Figure 2 shows LDM according to the x-y, x-z, and y-z planes. The mesh is subdivided in two parts: mesh for the closed room (zone 1) and mesh for the corridor (zone 2).

2.6 Ventilation scenarios

Three ventilation scenarios are used. In the first scenario, the isolated room is supplied with fresh air by two square diffusers measuring 0.6 m. The diffusers are at the sides of the room and are located in the ceiling. The air is extracted from the room by two square grilles also measuring 0.6 m and also positioned at the sides of the room and located in the ceiling. The objective of this strategy is to dilute the

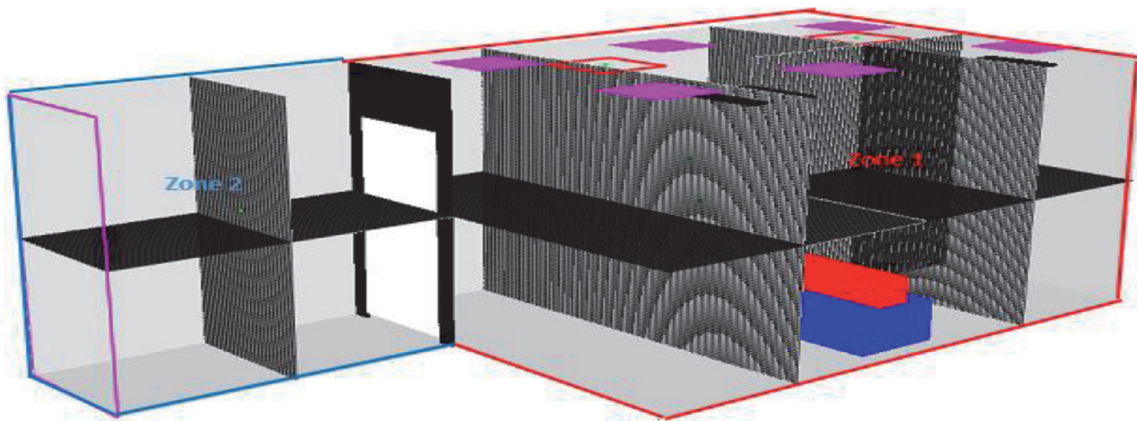


Figure 2.
LDM mesh.

contaminant as effectively as possible in order to obtain a uniform concentration of sulfur hexafluoride (SF6) across the entire volume of the room. In the first scenario, the contaminant is released in the room at a flow rate of 0.31 L/min. Numerically, we impose the release of the contaminant evenly on the six sides of a cube of 27 cm³ as a condition. We obtain the flow volume by a surface unit of $0.97 \times 10^{-3} \text{ m}^3$. Cheong and Phua [1] present some numerical and experimental results for the first scenario, which we demarcate as “scenario 1.”

In “scenario 2” the diffusers’ positions are similar to those in scenario 1. However, the air is extracted by two mural grilles located 30 cm above the floor near the patient’s bed. In this scenario, SF6 is released at a rate of 0.63 l/min ($1.94 \times 10^{-3} \text{ m}^3/\text{s/m}^2$). This second ventilation strategy aims at creating a flow from the top of the room to the floor. The aim is to quickly direct the gaseous contaminant “rejected” by the patient towards the extraction grilles. Numerically, it is very difficult to simulate the structure to the output of a diffuser of flow.

“Scenario 3” is similar to scenario 2, except that the supplying diffusers are replaced by blow grilles located on the ceiling directly above the patient. Unlike the diffusers, the air in scenario 3 is blown directly to the floor.

The component positions of the modeled room are presented in the table below.

3. Results and discussion

3.1 Scenario 1: Results and discussion

In the first ventilation scenario, two different software (FDS and Smokeview) allow the exploitation of a quantity of information at the end of every simulation. In this study, our attention is focused on the average concentrations of SF6 in the closed room and the spatial and temporal distribution of the concentration of SF6. Air velocity flow and temperature are also part of the reserved results (**Tables 2 and 3**).

Type of grid	Number of nodes
Dense mesh (DM)	3,218,400
Less dense mesh (LDM)	1,327,500
Coarse mesh (CM)	442,500

Table 2.
Number of nodes for each mesh.

Equipment	Positions (m)					
	Xmin	Xmax	Ymin	Ymax	Zmin	Zmax
Bed	1.40	3.20	2.05	2.75	0.0	0.40
Patient	1.50	3.15	2.25	2.55	0.40	0.65
Door	0.15	1.05	−0.02	0.00	0.05	2.00
Lamp 1	0.40	1.00	0.40	1.00	2.50	2.50
Lamp 2	2.20	2.80	0.40	1.00	2.50	2.50
Lamp 3	2.20	2.80	2.10	2.70	2.50	2.50
Lamp 4	0.40	1.00	2.10	2.70	2.50	2.50
Lamp 5	2.20	2.80	4.20	4.80	2.50	2.50
Lamp 6	0.40	1.00	4.20	4.80	2.50	2.50
Plaque 1	2.40	3.00	1.05	1.65	2.40	2.43
Plaque 2	2.40	3.00	3.65	4.25	2.40	2.43
Supply diffuser 1 (scenario 1) and (scenario 2)	2.40	3.00	1.05	1.65	2.50	2.50
Supply diffuser 2 (scenario 1) and (scenario 2)	2.40	3.00	3.65	4.25	2.50	2.50
Exhaust grille 1 (scenario 1) and supply diffuser 1 (scenario 3)	1.00	1.60	3.65	4.24	2.50	2.50
Exhaust grille 1 (scenario 1) and supply diffuser 2 (scenario 3)	1.00	1.00	1.00	1.60	2.50	2.50
Exhaust grille 1 (scenario 2) and (scenario 3)	2.40	2.90	4.80	4.80	0.40	1.00
Exhaust grille 2 (scenario 2) and (scenario 3)	2.40	2.90	2.40	2.40	0.40	1.00

Table 3.
Component positions of modeled room, supply diffuser, and exhaust grille in each scenario.

The results of scenario 1 are presented in **Tables 4** and **5**. As can be seen, the tables show a comparison between concentrations simulated by FDS and those simulated by Cheong and Phua [1]. The concentration simulated by FDS [C_{FDS}] and the experimental concentrations obtained by Cheong and Phua [1] [C_{exp}] are presented, respectively, in **Table 4**.

Error expressed as a percentage is given by $|([C_{FDS}] - [C_{exp}])/[C_{exp}]|$ for the concentration and by $|([V_{FDS}] - [V_{ex}])/[V_{ex}]|$ for the air velocity.

The concentrations obtained at points SP1, SP2, SP3, and SP5 by the LES code are inferior to the experimental results of Cheong and Phua [1]. These low concentrations can partly be explained by the infiltration of air under the door. Although Cheong and Phua [1] do not specify this infiltration rate or the pressure difference between the corridor and the closed room, AIA recommends that, for an operating room maintained at negative differential pressure, air flow to the extraction outlets must be 10% higher than the permitted air flow rate. In this case, the flow rate is

	SP1	SP2	SP3	SP4	SP5
[C_{FDS}]	20.00	22.50	20.40	34.20	28.60
Cheong and Phua [C_{exp}]	28.9 ± 0.7	28.0 ± 0.5	28.2 ± 0.6	33.4 ± 1.7	32.9 ± 0.9
Error (%)	31	20	28	2	10

Table 4.
SF6 concentration (ppm) simulated by FDS and Cheong and Phua [1].

	SP1	SP2	SP3
V _{FDS} (m/s)	0.15	0.15	0.12
V _{ex} (m/s)	0.14 ± 0.1	0.18 ± 0.2	0.16 ± 0.2
Error (%)	7	17	25

Table 5.
Air velocity simulated by FDS and Cheong and Phua [1].

14% higher than the blowing rate. Since the infiltration rate is slightly higher than recommended, the gaseous contaminant dilution will tend to be more efficient. This will lead to an average concentration of SF6 in the room, which is inferior to that obtained at a lower infiltration rate.

Table 5 shows both the simulated and experimental flow velocity modules, expressed in m/s. The V_{FDS} represents the average air velocity by the FDS over a range of 200 s (800–1000 s). In contrast, V_{ex} is the experimental air velocity in Cheong and Phua’s [1] study. As can be seen, there is excellent correlation between what is simulated by both methods and what is simulated by Cheong and Phua [1]. The deviations, shown as percentages, appear to be high and are expressed in cm/s. Specifically, they are less than 5 cm/s, which is not significant.

3.2 Scenarios 2 and 3: results

The concentrations obtained for scenarios 2 and 3 are presented in the following table.

Although FDS predicts a concentration that is slightly lower than the numerical code used by Cheong and Phua [1], the results obtained by FDS in scenario 2 are in agreement with those estimated by the researchers. On the other hand, considerable error is observed for scenario 3, in which the room is supplied with fresh air by two grids located on the ceiling. These grids tend to force the air to the floor. Points SP1 and SP3 are directly under the grids, and the concentration of SF6 is very low (<1 ppm). In this context, it is surprising that Cheong and Phua [1] obtained a concentration of 29.0 ppm at these points, as the only possible explanation would be related to the position of the supply grids. Although a plan of the room in Cheong and Phua’s [1] article seems to indicate that the supply grids are located directly under points SP1 and SP3, there is no information on the exact positioning of the grids (**Tables 6 and 7**).

Moreover, Cheong and Phua [1] do not give the recommended air temperature for the room. If the supply air temperature is high, then the Archimedes thrust will tend to significantly decrease the range of the jet. The influence of the blowing

Position	Scenario 2			Scenario 3		
	C _{FDS}	Cheong and Phua. [C.num]	Error (%)	C _{FDS}	Cheong and Phua. [C.num]	Error (%)
SP1	32.0	29.0	10	~0	29.0	10.0
SP2	28.4	34.0	18	21.2	28.0	24.0
SP3	27.3	30.5	11	~0	29.0	100.0

Table 6.
Numerical and simulated concentration (ppm) results.

Position	Scenario 2		Scenario 3	
	PREFDS	PRECheong and Phua	PREFDS	PRECheong and Phua
SP1	1.00	1.08	∞	1.08
SP2	1.13	0.91	1.22	1.12
SP3	1.17	1.03	∞	1.08

Table 7.
Pollutant removal efficiency.

temperature was checked through the increase by 2°C in the air temperature admitted into the room. The concentrations obtained at SP1 and SP3 remained negligible, which indicates that much higher temperatures would be required to reduce the range of the jets to a few tens of cm.

The flow velocity achieved a value of 0.05 m/s in nearly the entire room, except for the floor, where the velocity reached a value of 0.8. At the level of the diffusers, the air velocity was 0.6 m/ s. Further, it was observed that the jet of air coming from the corridor faded before reaching the other end of the room. This jet of air diffused in the vertical direction, which helped to dilute the gaseous contaminant in the room.

The influence of the blowing grids on the concentrations is clearly visible. As mentioned earlier, very significant changes in concentration are observed in the area above the patient’s bed. A slight change in the position of the blown grids is likely to have a significant impact on the simulated concentrations at SP1 and SP3. Point SP2, which is situated at the foot of the patient’s bed, is in an area where variations in concentration are less important.

3.3 Pollutant removal efficiency index

In order to compare the effectiveness of the three ventilation strategies, the pollutant removal efficiency (PRE) index is used.

PRE is calculated as follows:

$$PRE = \frac{C_s}{C_j} \tag{7}$$

where C_s is the average concentration of SF6 in the exhaust air grille; C_j is the average concentration of SF6 at points (x, y, z).

The PRE can be calculated for a room with more exhaust grilles by averaging the concentrations obtained at the various extraction grids. The PRE index is used to quantify the effectiveness of ventilation to remove pollutants from a room. It depends on a number of factors, such as the location of the source of the pollutant, the supply flow, the ventilation strategy, etc. The strategy is effective for removing pollutants and represents a good ventilation solution if $PRE > 1$. On the other hand, if $PRE < 1$, there is an accumulation of contaminants in the room. This could be related to, for example, the existence of recirculation zones where the contaminants accumulate.

For scenario 2 in the three points of SP1, SP2, and SP3, we obtain $PRE > 1$. This result is the same as that in Cheong and Phua’s [1] work, except for SP2. In scenario 3, the FDS simulation gives completely different results than Cheong and Phua’s [1] for the two points of SP1 and SP3.

4. Conclusions

This paper investigated the air quality in a bronchoscopy unit. The numerical model used in the present study was based on the large-eddy simulation (LES) method. The numerical results obtained in this work have been generally validated by the experimental results found in the literature. For this investigation, we used Cheong and Phua's [1] study for validation and comparison purposes. Three numerical scenarios (scenario 1, scenario 2, and scenario 3) were developed according to ASHRAE norms and standards. Fire Dynamics Simulator software was used to estimate the concentration of contaminants and the air velocity in the bronchoscopy unit. According to the results obtained, both scenario 1 and scenario 2 are effective for removing SF₆ (pollutants). However, according to our results, scenario 3 should not be retained, as in this scenario, the concentration of pollutants was very high compared to the other two scenarios. Moreover, the concentration of SF₆ accumulated around the patient's bed.

In light of these findings, the authors of the present work suggest that more in-depth investigation into the air quality of hospitals is warranted. This could be combined with field experiments using scenarios 1 and 2.

Author details

Hanaâ Hachimi¹, Chakib El Mokhi², Badr T. Alsulami³ and Abderrahim Lakhout^{4*}

¹ Sultan Moulay Slimane University, Beni Mellal, Morocco

² National School of Applied Sciences, Ibn Tofail University, Kenitra, Morocco

³ Department of Civil Engineering, College of Engineering and Islamic Architecture, Umm Al-Qura University, Saudi Arabia

⁴ Civil Engineering Department, Faculty of Engineering, University of Tabuk, Saudi Arabia

*Address all correspondence to: a.lakhout@usherbrooke.ca

IntechOpen

© 2020 The Author(s). Licensee IntechOpen. This chapter is distributed under the terms of the Creative Commons Attribution License (<http://creativecommons.org/licenses/by/3.0>), which permits unrestricted use, distribution, and reproduction in any medium, provided the original work is properly cited. 

References

- [1] Cheong KWD, Phua SY. Development of ventilation design strategy for effective removal of pollutant in the isolation room of a hospital. *Building and Environment*. 2006;**41**(9):1161-1170
- [2] Sundell J. On the history of indoor air quality and health. *Indoor Air*. 2004;**14**(s7):51-58
- [3] Kuehn TH. Airborne infection control in health care facilities. *Transactions-American Society of Mechanical Engineers Journal of Solar Energy Engineering*. 2003;**125**(3): 366-371
- [4] Dales R, Liu L, Wheeler AJ, Gilbert NL. Quality of indoor residential air and health. *Canadian Medical Association Journal*. 2008;**179**(2): 147-152
- [5] Jones AP. Indoor air quality and health. *Atmospheric Environment*. 1999;**33**(28):4535-4564
- [6] Sautour M, Sixt N, Dalle F, L'Ollivier C, Fourquenot V, Calinon C, et al. Profiles and seasonal distribution of airborne fungi in indoor and outdoor environments at a French hospital. *Science of the Total Environment*. 2009; **407**(12):3766-3771
- [7] Lakhout A. Modélisation de la qualité de l'air dans une unité de bronchoscopie: influence des stratégies de ventilation. 2011. Thèse de doctorat. École de technologie supérieure
- [8] Saad SG. Integrated environmental management for hospitals. *Indoor and Built Environment*. 2003;**12**(1-2):93-98
- [9] De Giuli V, Zecchin R, Salmaso L, Corain L, De Carli M. Measured and perceived indoor environmental quality: Padua hospital case study. *Building and Environment*. 2013;**59**:211-226
- [10] Pittet D, Allegranzi B, Sax H, Bertinato L, Concia E, Cookson B, et al. Considerations for a WHO European strategy on health-care-associated infection, surveillance, and control. *The Lancet Infectious Diseases*. 2005;**5**(4): 242-250
- [11] Hathway A, Noakes CJ, Sleigh PA. CFD modeling of a hospital ward: Assessing risk from bacteria produced from respiratory and activity sources. In: *Indoor Air 2008: The 11th International Conference on Indoor Air Quality and Climate*. Leeds; Indoor Air 2008, 17-22nd August 2008, Copenhagen, Denmark
- [12] Qian H, Li Y. Removal of exhaled particles by ventilation and deposition in a multibed airborne infection isolation room. *Indoor Air*. 2010;**20**(4): 284-297
- [13] McGrattan K, Hostikka S, McDermott R, Floyd J, Weinschenk C, Overholt K. *Fire Dynamics Simulator, User's Guide*. 6th ed. National Institute of Standards and Technology: NIST Special Publication; 2013. p. 1019
- [14] Barrero D, Hardy J-P, Reggio M, Ozell B. CFD and realistic visualization for the analysis of fire scenarios. In: *ACM SIGGRAPH 2004 Posters*. ACM; 2004. p. 101
- [15] Temam R. *Navier-Stokes Equations*. Vol. 2. North-Holland Amsterdam; 1984
- [16] Persily A. Challenges in developing ventilation and indoor air quality standards: The story of ASHRAE standard 62. *Building and Environment*. 2015;**91**:61-69